A mathematical model for *Plasmodium vivax* malaria transmission: estimation of the impact of transmission-blocking immunity in an endemic area

A.P.K. De Zoysa,[1] C. Mendis,[2] A.C. Gamage-Mendis,[2] S. Weerasinghe,[3] P.R.J. Herath,[4] & K.N. Mendis[5]

We have developed a multi-state mathematical model to describe the transmission of Plasmodium vivax *malaria; the model accommodates variable transmission-blocking/enhancing immunity during the course of a blood infection, a short memory for boosting immunity, and relapses. Using the model, we simulated the incidence of human malaria, sporozoite rates in the vector population, and the level of transmission-blocking immunity for the infected population over a period of time. Field data from an epidemiological study conducted in Kataragama in the south of Sri Lanka were used to test the results obtained. The incidence of malaria during the study period was simulated satisfactorily. The impact of naturally-acquired transmission-blocking immunity on malaria transmission under different vectorial capacities was also simulated. The results show that at low vectorial capacities, e.g., just above the threshold for transmission, the effect of transmission-blocking immunity is very significant; however, the effect is lower at higher vectorial capacities.*

Introduction

Malaria transmission-blocking immunity that is mediated by serum antibodies against the sexual stages (gametes and zygotes) of the malaria parasite occurs in the midgut of the mosquito vector and arrests further development of the parasite in the insect. This immunity was first described following its induction in animals by artificial immunization (*1*, *2*), and subsequently in humans as a response to natural malaria infections (*3–5*). Increasing the level of antibodies to reduce parasite infectivity has been developed as a potential vaccine strategy against the human malarias. Transmission-blocking vaccines differ from others in that they aim primarily to reduce the reservoir of infection in an endemic community, as opposed to directly protecting the vaccinated individual. The impact of such vaccines on malaria in a community therefore depends to a much greater extent on the dynamics of transmission than with vaccines against other stages of the malaria parasite. It is therefore more difficult to assess intuitively the impact of transmission-blocking vaccines on disease incidence. Quantitative studies are thus needed to ascertain the potential impact of reducing infectivity and to determine the extent to which this depends on the prevailing intensity of transmission.

We have previously used mathematical studies to quantify the effects of naturally-acquired transmission-blocking immunity on malaria. In this way, using field data from a *Plasmodium vivax* epidemic that occurred in a region of Sri Lanka, we showed that naturally-acquired transmission-blocking immunity can lead to a significant reduction in the incidence of malaria during an epidemic (*6*). This was the first attempt to model *P. vivax* transmission and to simulate explicitly the evolution and effects of transmission-blocking immunity. However, the method could not predict immunity levels, values for which had to be derived from field observations; the procedure therefore was of little value for quantifying transmission in other settings.

In the present article we report a comprehensive mathematical model for *P. vivax* malaria that takes into account transmission-blocking immunity in humans, including the boosting of immunity by repeated infections, and a defined and short immune memory for boosting. The model was developed and tested using field and laboratory data collected in an

[1] Senior Lecturer and Head, Division of Mathematics and Philosophy of Engineering, Open University of Sri Lanka, P.O. Box 21, Nugegoda, Sri Lanka. Requests for reprints should be sent to this author.

[2] Research Scientist, Malaria Research Unit, Department of Parasitology, Faculty of Medicine, University of Colombo, Colombo, Sri Lanka.

[3] Technician, Malaria Research Unit, Department of Parasitology, Faculty of Medicine, University of Colombo, Colombo, Sri Lanka.

[4] Scientist, Malaria Control Unit, World Health Organization, Geneva, Switzerland.

[5] Associate Professor, Malaria Research Unit, Department of Parasitology, Faculty of Medicine, University of Colombo, Colombo, Sri Lanka.

Reprint No. **5229**

© World Health Organization 1991

epidemiological study in which malaria transmission was monitored for two consecutive peak transmission periods in Kataragama, an area in the south of Sri Lanka that is endemic for *P. vivax* malaria (*7*). Since the model was developed with the specific aim of predicting the levels of naturally-acquired transmission-blocking immunity in the population, and of assessing its effect on malaria transmission, it could be used to evaluate different control strategies for *P. vivax* malaria.

Materials and methods

General description of the model

Based on an approach described by Dietz et al. (*8*) for *P. falciparum*, we have developed a multi-state mathematical model for *P. vivax*. The model represents 21 states that consider negative (uninfected), incubating, and blood-positive (infected) stages of *P. vivax* malaria in humans. Up to two relapses (with one or two broods of hypnozoites are accommodated and two levels of transmission-blocking immunity: level-1 for a primary infection and a boosted level-2 for a post-primary infection. A variable infectivity of the parasite to mosquitos during the course of a human infection was modelled, based on transmission-enhancing and transmission-blocking antibodies (*9*). The model and the transfer rate equations between the different states and levels of immunity are shown schematically in Fig. 1 and described in detail in Annex 1.

An explicit vector model was used, assuming that no recovery or superinfection was possible. The man–mosquito contact rate was taken to be homogeneous and a Poisson distribution was used to

Fig. 1. **Scheme showing the transfers (inoculation, recovery and immune loss, relapse, and incubation) between the 21 states of infection and recovery used in the model.** The states are denoted as follows: Z = the number in negative uninfected states; X = the number in incubating states (pre-infective states); and Y = the number in positive infective states. The first subscript on X, Y or Z indicates the level of transmission-blocking immunity; the second indicates the number of hypnozoite broods in the liver, e.g., $Z_{1\,2}$ denotes an uninfected human with an immunity at level-1 and two broods of hypnozoites in the liver. The states are numbered 1–3 for level-0, 11–19 for level-1, and 21–29 for level-2. The equations governing these states are described in Annex 1.

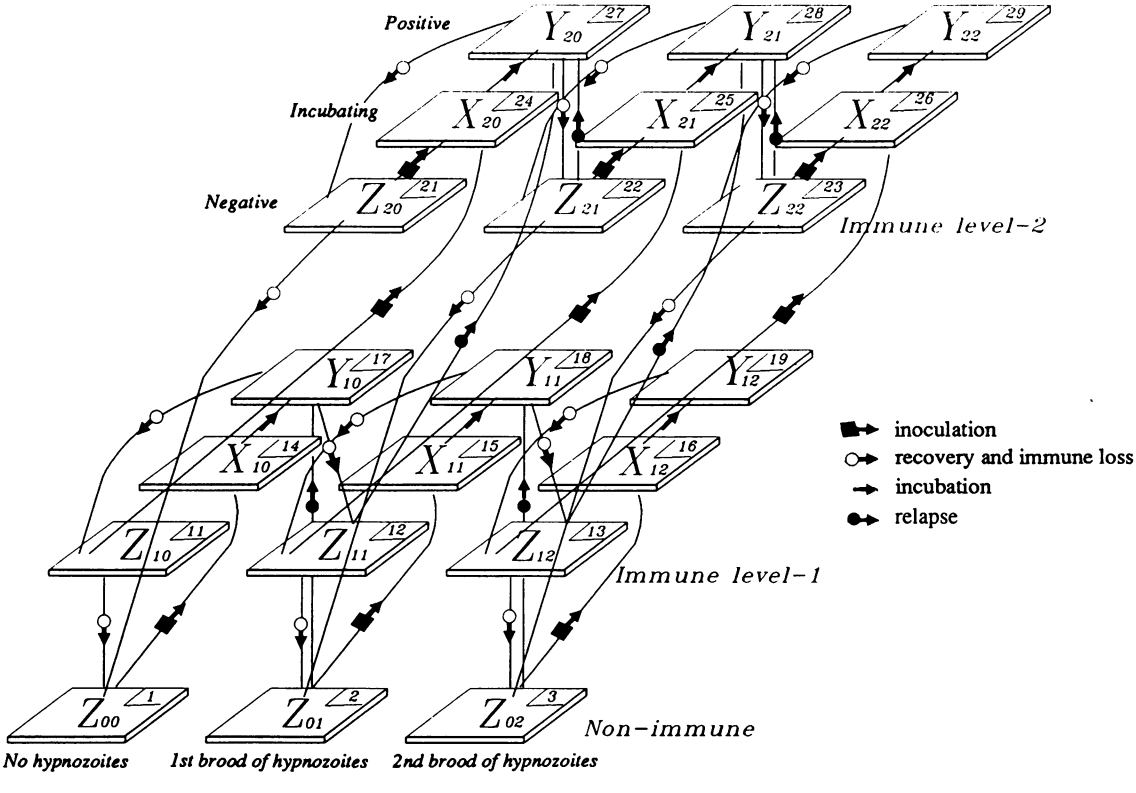

Fig. 2. **Scheme showing the transfers between the three vector states used in the model.** The equations governing these states are described in Annex 2.

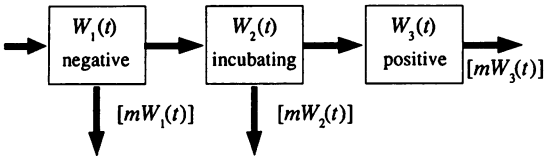

determine the expected contact rates (see Fig. 2 and Annex 2).

Transmission-blocking immunity and infectivity

Natural malaria infections in humans lead to the production of antibodies directed against the surface antigens of the malaria parasite gametes. At sufficiently high concentrations these antibodies reduce the infectivity of the parasite to mosquitos (*3*) and at lower concentrations have the opposite effect, i.e., enhance its infectivity (*10*). Transmission-blocking immunity was modelled on the basis that serum from the early stages of a primary infection, when antibody titres are low, enhances infectivity, while that from the latter stages, when titres are high, blocks transmission (Fig. 3) (*9*). This immunity is evoked even by a primary malaria infection (level-1 immunity) (*3*), and can be boosted by subsequent infections (level-2 immunity) if they occur within approximately 4 months of the previous infection, i.e., the immune memory for boosting the response is completely lost unless reinfection occurs within 4 months (*4*).

We assumed that the infectivity of patients varies only as a result of transmission-blocking or transmission-enhancing immunity and that the average duration of a potentially infective period of an infection (gametocyte positive) is 4 days. This relatively short infection period means that a significant contact rate is necessary to sustain transmission, and hence we observed a high threshold vectorial capacity.

Fig. 3. **Curve showing the relative infectivity of a patient over time, as assumed in the model.** N_Γ and f are defined in the text (see section "Modelling infectivity"). The 100% relative infectivity corresponds to a level of infectivity without transmission blocking or enhancement.

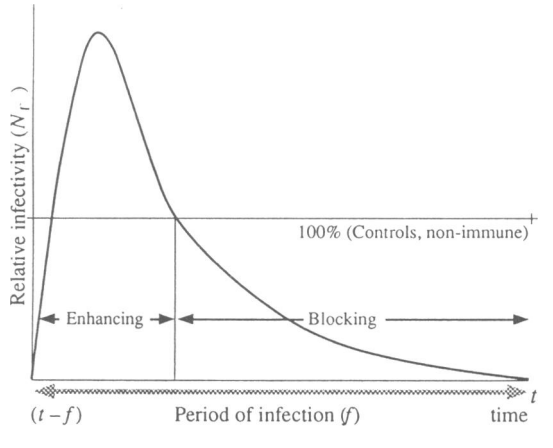

Modelling infectivity

The relative infectivity was defined as the probability of a mosquito developing sporozoites from biting a patient relative to that of developing sporozoites from a similar bite, in the absence of transmission-blocking or transmission-enhancing immunity.

Fig. 3 depicts the typical relative infectivity variation, N_Γ, relative to the duration of a blood infection, where Γ is the level of immunity (1 or 2), and f the period of infectivity. If the number of new arrivals at time η is $\Omega(\eta)$ and M is the proportion of positives who are infective, the average relative infectivity per individual at time t for a positive state in the population, $Y_{\Gamma j}$, at level Γ of immunity is given by:

$$I_{\Gamma j}(t) = M \int_{(t-f)}^{t} N_\Gamma(t-\eta)\Omega_{\Gamma j}(\eta)\mathrm{d}\eta \Big/ \int_{(t-f)}^{t} \Omega_{\Gamma j}(\eta)\mathrm{d}\eta \quad (A)$$

where $(t-f) \leq \eta \leq t$; for $j = 1$–3.

The relative infectivity, $I_{\Gamma j}$, could take one of two levels corresponding to transmission-blocking immunity with ($\Gamma = 2$) or without ($\Gamma = 1$) boosting. Values for the relative infectivity on days 1–4 after infection are given in Table 1.

The serum effects on variation in infectivity, relative to non-immune serum, for the first 4 days of infection are also shown in Table 1. These values were derived from measurements of transmission-blocking immunity made on sera of *P. vivax* patients during the study (A. C. Gamage-Mendis et al., unpublished results, 1991). The average individual relative infectivity, $J_\Gamma(t)$, in the human population at time t and immune level Γ is given by

$$J_\Gamma(t) = \sum_{j=0}^{2} I_{\Gamma j}\, Y_{\Gamma j}(t) \Big/ \sum_{j=0}^{2} Y_{\Gamma j}(t) \quad (B)$$

for $\Gamma = 1, 2$.

Table 1: **Relative infectivity used by the model for patients infected with *Plasmodium vivax* malaria**[a]

No. of days after infection	Infectivity relative to non-immune controls: $N_1(\eta)$[b]	$N_2(\eta)$[c]	Effect on infectivity
1	2.58	1.20	Enhancing
2	0.6	0.29	Blocking
3	0.23	0.03	Blocking
4	0.013	0.0	Blocking
Average	0.86	0.38	—

[a] Infectivity of individuals without enhancement or blocking = 1.
[b] Level-1.
[c] Level-2, boosted.

Modelling immune memory for boosting

A negative (uninfected) state (k) with immune memory and the rate equation for the state [k] are shown schematically below

$$ZI(t) \rightarrow \boxed{\begin{array}{c} Z(t) \\ \text{state } [k] \end{array}} \rightarrow ZO(t)$$

$$\downarrow$$

$$\Theta(t)Z(t)$$

where $Z(t)$ = the total number of individuals occupying the state [k]; $ZI(t)$ = the daily rate of entry to this state; $\Theta(t)$ = daily probability of a reinfection (due to inoculation or relapse) in this state; and $ZO(t)$ = the daily rate of removal from this state with loss of immune memory = μ_k, as defined in Fig. 1.

It can be shown that

$$d(Z(t))/dt = ZI(t) - \Theta(t)Z(t) - ZO(t) \qquad (C)$$

$ZO(t)$ is the proportion of individuals who entered the immune state at time $(t - T)$, where T is the period after which there is a complete loss of immune memory for boosting.

To derive an expression for $ZO(t)$, we shall follow a set of individuals, $ZI(t - T)$, who first entered the immune state on day $(t - T)$. Let the number of individuals who entered this state on day $(t - T)$ and who remain after time ϕ has elapsed be $\widehat{ZI}(t - T, \phi)$, where $0 < \phi < T$.

Since

$$d(\widehat{ZI}(t - T, \phi))/d\phi = -\Theta(t - T + \phi)\widehat{ZI}(t - T, \phi),$$

$$\int_0^T d(\widehat{ZI}(t - T, \phi))/\widehat{ZI}(t - T, \phi) = -\int_0^T \Theta(t - T + \phi)\, d\phi$$

which, after integrating gives

$$\widehat{ZI}(t - T, T) = \widehat{ZI}(t - T, 0) \times \exp\left[-\int_0^T \Theta(t - T + \phi)\, d\phi\right].$$

Since $\widehat{ZI}(t - T, T)$ is the number of individuals who entered the state at time $(t - T)$ and who are still there at time t,

$$\widehat{ZI}(t - T, T) = ZO(t)$$

and

$$\widehat{ZI}(t - T, 0) = ZI(t - T).$$

If we define

$$T \times \Theta^*(t) = \int_0^T \Theta(t - T + \phi)\, d\phi,$$

where $\Theta^*(t)$ is the average rate of removal from $(t - T)$ to t, then

$$ZO(t) = ZI(t - T) \exp[-\Theta^*(t)T] = \mu_k \qquad (D)$$

which upon substitution in (C), gives

$$(dZ(t)/dt) = ZI(t) - \Theta(t)Z(t) - ZI(t - T) \exp[-\Theta^*(t)T] \qquad (E)$$

The terms in eq. E for the different k states are given in Annex 3, while the states themselves are shown in Fig. 1.

Vector model

Epidemiological studies have determined that six of the anopheline species prevalent in the study area are infected with the sporozoites of human malarias (*7*). In order to simplify the modelling of the vector, we adjusted the man-biting rate of each of these species with reference to that of *Anopheles culicifacies*, the best-studied malaria vector in Sri Lanka, using a relative transmission efficiency factor whose derivation has been described elsewhere (*16*). In the simulations we used the properties of a single *A. culicifacies* vector in conjunction with the "effective" man-biting rates of the other species.

The model is shown schematically in Fig. 2 and described in detail in Annex 2.

Simulating the Kataragama epidemic

The set of coupled first-order differential equations shown in Annex 1 was solved numerically on a microcomputer using a program in PASCAL and the transmission of *P. vivax* malaria was simulated for the 17 months of the field study. To establish

transmission-blocking immunity levels at the start of the simulation, we required information about the inoculation history of individuals prior to the monitoring period. We therefore started the simulation 4 months before the period of monitoring began, using the monthly *P. vivax* incidence recorded at Kataragama by the national antimalaria campaign, and estimated the man-biting rate during this period by assuming that this rate lagged behind the incidence by 1 month and that the incidence was proportional to the man-biting rate.

We then computed the incidence for the first 4 months of the field study (November 1986 to February 1987), which corresponded to the first peak transmission period. The values S, S_0 and S_1 defined in Annexes 1 and 2 were varied until the simulated values agreed closely with the observed incidence over these 4 months (least squares difference). The search for a solution was limited to values of S, S_1 and S_0 between 0 and 1. We obtained a unique solution for S, S_0 and S_1 by ensuring that the predicted daily prevalence, sporozoite rate, and level of immunity agreed closely with the observed levels. The simulation was then extended to the entire monitoring period, i.e., up to March 1988, which included a period of low transmission (April–September 1987) and a second peak transmission period (October 1987 to March 1988). A higher man-biting habit was used for the 6 months during the dry season than for the wet season, as has been observed for Sri Lanka (P.R.J. Herath, unpublished results, 1988).

Results

The simulated monthly incidence of malaria (with transmission-blocking immunity) shown in Fig. 4 agrees reasonably well with the observed incidence. To estimate the effect of transmission-blocking immunity on the incidence, we performed the simulation in the absence of immunity, i.e., by assuming that the relative infectivity of all infective individuals was 1.0. This resulted in a much higher incidence throughout the monitoring period (Fig. 5a). The effect of boosting immunity by repeated infection was investigated by performing the simulation with equal relative infectivity values for immune level-1 and level-2; boosting appeared to have a substantial impact on the infectivity of patients and hence on transmission (Fig. 5b).

Table 2: **Effect of immunity on the incidence of *Plasmodium vivax* malaria**

Category	% of patients: Observed	Simulated: With immunity	Simulated: Without immunity
Primary infections or repeat infections beyond 4 months	85.9	84.4	61.2
Repeat infection within 4 months	14.1	15.6	38.9

The immune status of the population determined from the field data and given by the simulation are very similar (Table 2). The average daily prevalence of *P. vivax* predicted by the simulation was 0.08% in the presence, and 1.13% in the absence of immunity.

The effect of transmission-blocking immunity at different vectorial capacities (vectorial capacity as

Fig. 4. **Monthly incidence of *Plasmodium vivax* malaria as observed during the epidemiological study and simulated (accounting for transmission-blocking immunity), together with the man-biting rate measured during the study.**

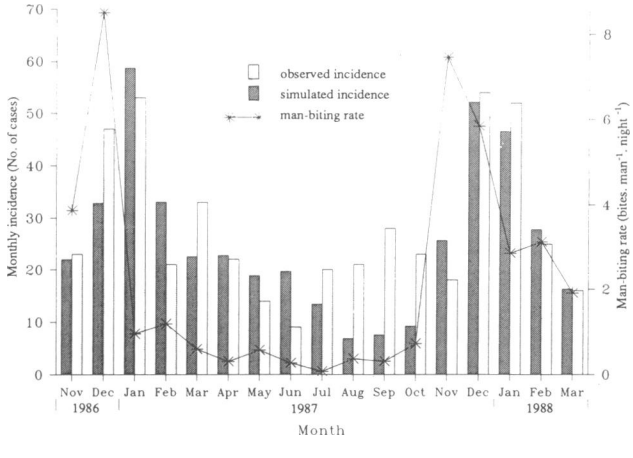

Fig. 5. a) **Simulated monthly incidence of *Plasmodium vivax* malaria with and without transmission-blocking immunity and** b) **with transmission-blocking immunity in the presence and absence of boosting. The simulated monthly average individual relative infectivity of patients in the absence and presence of boosting is also shown.**

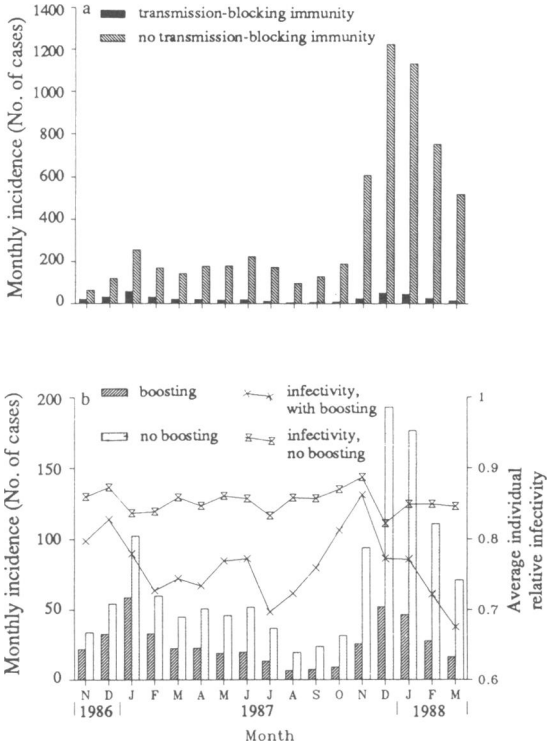

Fig. 6. **Variation of the incidence of *Plasmodium vivax* malaria expressed as a proportion of the total population, with vectorial capacity in the presence and absence of transmission-blocking immunity, as simulated by the model. The simulations were performed for 400 days at each vectorial capacity.**

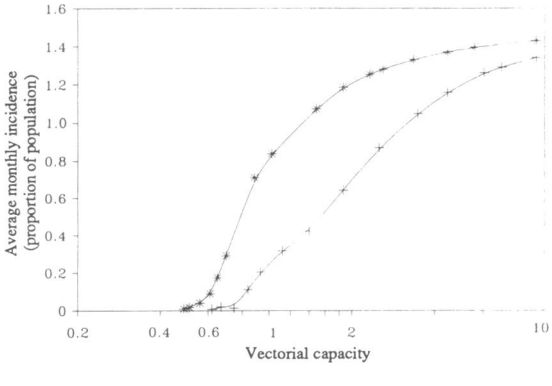

defined in Dietz et al. (*8*)) was calculated by determining the monthly incidence reached when the vectorial capacity was held constant for a sufficiently long period of time, with or without transmission-blocking immunity (Fig. 6). The effect of transmission-blocking immunity was most marked at low vectorial capacities. In Kataragama the predicted threshold vectorial capacity to sustain transmission was 0.63 with transmission-blocking immunity, and 0.49 without. The vectorial capacity during the study period varied from 0.07 to 1.4.

No account was taken of a concurrent *P. falciparum* epidemic that occurred in the study region during the period of the field study (*7*).

Discussion

The mathematical model that we have described to simulate transmission of *P. vivax* malaria in humans incorporates naturally-acquired transmission-blocking immunity and was used in conjunction with data obtained from a field study to simulate the transmission during two consecutive seasons in an area that is endemic for malaria in Sri Lanka.

The results of the simulation agreed well with the observed incidence of *P. vivax* malaria, particularly during the high transmission periods. However, during the dry season when transmission was low, the simulated incidence fell below the observed (July–October 1987). This discrepancy may have been due to the following: during the dry season the human blood index in the vector often increases because cattle migrate away from areas of human habitation (in the simulation a correction for this had to be estimated); clustering of malaria infections in the human population because of non-homogeneous inoculations (*11*)—in contrast we assumed homogeneity; and inaccuracies in the measurements of the man-biting rate in the dry season because of very low vector densities. The generally low entomological inoculation rates that prevail in Sri Lanka (*7*) made the simulation extremely sensitive to the decisive parameters, such as the man-biting rate, habit and vector mortality. The monthly average incidence of *P. vivax* malaria, even during peak transmission periods, was as low as 1.5% and man-biting rates were about 8 bites per person per night. As we have shown, the threshold vectorial capacity to sustain transmission was 0.63. In Kataragama the vectorial capacity varied from 0.07 to 1.4, indicating that transmission during the study period had been sustained at a level only marginally above the threshold. This is in contrast to most simulations of malaria transmission reported by other workers; for example, in Garki, where the vectorial capacities were well above the threshold values required to

sustain transmission (*12*). In Garki, the peak vectorial capacities were nearly 1000 times the threshold value, while in Kataragama the peak values were only 2–3 times the threshold and were lower than the threshold for 6 months of the year. In situations where the incidence of human malaria is very low and involves clusters of small groups, such as occurred in Kataragama during the dry season, stochastic models might be more appropriate than the deterministic formulation we have used here (*13*, *14*).

Our model accounts for several unique features that influence transmission of *P. vivax* malaria, such as relapses from up to two broods of hypnozoites, and all known features of transmission-blocking immunity; these include a variation of immunity during the course of a patent blood infection, and its boosting subject to reinfection within a short period. We have, however, explicitly not modelled immunity to other stages of the malaria parasite. Immunity to the anti-asexual stage would have lowered the average infectivity of patients and reduced the proportion of the population susceptible to malaria; it was assumed that these would not vary much during a single transmission period if there was no appreciable change in the age distribution of the population. Therefore the factors S and S_0 used in the model would have accounted for these effects, albeit approximately.

The simulation shows that under the prevailing transmission conditions in Sri Lanka, the incidence of *P. vivax* malaria would have been significantly higher in the absence of naturally-acquired transmission-blocking immunity. It thus appears that despite the infectivity-enhancing effects of antigamete antibodies, the overall effect of immunity on an endemic population is to significantly reduce transmission of malaria. The model also showed that the boosting of immunity by frequent reinfection contributed significantly to lowering the infectivity of the population; the frequent boosting of immunity during the high-transmission season reduced infectivity during the following low-transmission season. Subsequently, the short immune memory for boosting, coupled with the low inoculation rates that prevailed during the dry season, led to a loss of immunity and a restoration of the original level of infectivity at the onset of the next transmission season. Transmission-blocking immunity, however, had little effect on the duration of the high-transmission season or on the temporal distribution of the incidence of malaria, i.e., the shape of the incidence curve, which was largely determined by vector densities.

The threshold vectorial capacity in Kataragama is much higher than that reported for the Garki project (*12*), largely because of the high recovery rates in Sri Lanka resulting from effective chemotherapy. In Kataragama transmission-blocking immunity raises the threshold vectorial capacity by about 30%, and the impact of this immunity becomes less pronounced as the vectorial capacity increases.

The model explicitly describes transmission-blocking immunity and has been tested in a situation where low intensities of transmission prevail; however, it can also be used to evaluate vector control methods and to simulate transmission-blocking vaccine trials in situations where different transmission characteristics occur.

Acknowledgements

We are very grateful to Dr L. Molineaux for valuable discussions and suggestions. We also thank J. Rajakaruna, M.U. Kularatne, R. Wimalagunaratne, N. Jayasena, P. Wanniarachchi, P. Sumanaweera and U. Mohotti for expert technical assistance, and A. Mahakumara, C. Marimuttu, R.A.D. Wasantha Kumara, K.L. Premasiri, A.H. Sunil, M.A. Abeywardene, R.P. Ariyasena, P. Palihakkara, and R. Jinadasa for their contributions to this study. The cooperation of the Director, Anti-malaria Campaign, Sri Lanka, and M.M. Ismail are gratefully acknowledged.

This investigation received financial support from the UNDP/World Bank/WHO Special Programme for Research and Training in Tropical Diseases.

Résumé

Transmission du paludisme à *Plasmodium vivax*: modèle mathématique pour estimer l'effet de l'immunité bloquant la transmission en secteur d'endémie

Les anticorps dirigés contre les stades sexués des plasmodies sont élaborés en réponse aux infections palustres naturelles et diminuent ou même neutralisent l'infectiosité pour le moustique vecteur des gamétocytes présents chez le patient. L'élévation du titre d'anticorps anti-stades sexués pour diminuer l'infectiosité du parasite a été envisagée parmi les stratégies vaccinales possibles contre les paludismes humains. L'immunité bloquant la transmission pourrait diminuer la transmission palustre dans les secteurs d'endémie. L'objet de la présente étude est de décrire un modèle mathématique appliqué à la transmission du paludisme à *P. vivax* et son utilisation pour quantifier les effets de l'immunité antipalustre bloquant la transmission acquise naturellement en secteur d'endémie. Le modèle tient compte des

caractéristiques suivantes de la transmission de *P. vivax*:

—immunité bloquant la transmission suscitée par une primo-infestation et immunité secondaire due à une réinfestation dans un délai donné;

—disparition de la mémoire immunitaire après une période donnée en l'absence de réinfestation;

—"activation" de l'infectiosité au début de l'infestation;

—rechutes résultant de l'existence de deux générations d'hypnozoïtes.

La modélisation a utilisé une méthode décrite pour la première fois par Dietz et al. pour *P. falciparum*. Le modèle recouvre 21 états, correspondant à trois stades: négatif (pas d'infestation), incubation, et positif (infestation); les rechutes et deux degrés différents d'immunité (réponse primaire et réponse secondaire) sont également pris en compte par le modèle. Un modèle vectoriel explicite qui suppose un contact aléatoire homogène est utilisé. L'ensemble des couples d'équations différentielles qui en résultent ont été numériquement résolus au moyen d'un ordinateur, et les résultats utilisés pour simuler la transmission du paludisme à *P. vivax* sur une durée de 17 mois à Kataragama, dans le sud du Sri Lanka, secteur où l'endémicité est faible. L'incidence palustre et le niveau de l'immunité bloquant la transmission simulés dans la population concordent relativement bien avec les valeurs observées.

Pour estimer l'effet de l'immunité bloquant la transmission sur l'incidence du paludisme, la simulation a été réalisée en l'absence d'immunité. Une incidence beaucoup plus élevée a alors été observée tout au long de la période de surveillance. L'effet de l'immunisation secondaire, à la suite d'une nouvelle infestation, a été étudié par la simulation en donnant à l'infectiosité relative des valeurs égales pour les deux niveaux immunitaires; le renforcement de l'immunité par des réinfestations fréquentes (ou des rechutes) semble avoir un impact considérable sur l'infectiosité des patients et, par conséquent, sur la transmission. A Kataragama, la transmission se maintient pour des capacités vectorielles relativement basses, c'est-à-dire à peine au-dessus du seuil. Les résultats de la simulation pour des capacités vectorielles différentes mais constantes, avec ou sans immunité, donnent à penser que l'effet de l'immunité sur la transmission est faible quand la capacité vectorielle est élevée.

Ces simulations amènent aux conclusions suivantes:

—L'immunité bloquant la transmission acquise naturellement peut jouer un rôle de régulateur dans la transmission du paludisme et diminuer considérablement l'incidence palustre dans un secteur de transmission.

—Les réponses immunitaires secondaires dues à des réinfestations fréquentes sont un facteur important dans la diminution de l'incidence palustre.

—L'immunité bloquant la transmission acquise naturellement est sans effet important sur la capacité vectorielle seuil, nécessaire au maintien de la transmission.

—L'immunité bloquant la transmission a un effet plus marqué sur l'incidence du paludisme quand la capacité vectorielle est faible, et un effet moindre quand la capacité vectorielle augmente.

References

1. **Carter, R. & Chen, D.H.** Malaria transmission blocked by immunization with gametes of the malaria parasite. *Nature*, **263**: 57–60 (1976).
2. **Gwadz, R.W.** Malaria: successful immunization against sexual stages of *Plasmodium gallinaceum*. *Science*, **193**: 1150–1151 (1976).
3. **Mendis, K.N. et al.** Malaria transmission-blocking immunity induced by natural infections of *Plasmodium vivax* in humans. *Infection and immunity*, **55**: 369–372 (1987).
4. **Ranawaka, M.B.R. et al.** Boosting of transmission blocking immunity during natural *Plasmodium vivax* infections in man depends upon frequent reinfection. *Infection and immunity*, **56**: 1820–1824 (1988).
5. **Graves, P.M. et al.** Naturally occurring antibodies to an epitope on *P. falciparum* gametes detected by monoclonal antibody-immunosorbant assay. *Infection and immunity*, **56**: 2818–2821 (1988).
6. **De Zoysa, A.P.K. et al.** Modulation of human malaria transmission by anti-gamete transmission-blocking immunity. *Transactions of the Royal Society of Tropical Medicine and Hygiene*, **82**: 548–553 (1988).
7. **Mendis, C. et al.** Characteristics of malaria transmission in Kataragama, Sri Lanka: a focus for immuno-epidemiological studies. *American journal of tropical medicine and hygiene*, **42**: 298–308 (1990).
8. **Dietz, K. et al.** A malaria model tested in the African savanna. *Bulletin of the World Health Organization*, **50**: 347–357 (1974).
9. **Naotunne, T. de S. et al.** *Plasmodium cynomolgi*: serum-mediated blocking and enhancement of infectivity to mosquitoes during infections in the natural host, *Macaca sinica*. *Experimental parasitology*, **71**: 305–313 (1990).
10. **Peiris, J.S.M. et al.** Monoclonal and polyclonal antibodies both block and enhance transmission of human *Plasmodium vivax* malaria. *American journal of tropical medicine and hygiene*, **39**: 26–32 (1988).
11. **Dye, C. & Hasibeder, G.** Population dynamics of mosquito-borne disease: effect of flies which bite some people more frequently than others. *Trans-*

actions of the Royal Society of Tropical Medicine and Hygiene, **80**: 67–77 (1986).

12. **Molineaux, L. & Gramiccia, G.** *The Garki project: research on the epidemiology and control of malaria in the Sudan savanna of West Africa.* Geneva, World Health Organization, 1980.
13. **Macdonald, G. et al.** The dynamics of malaria. *Bulletin of the World Health Organization,* **38**: 743–755 (1968).
14. **Bailey, N.T.J.** *The mathematical theory of infectious diseases.* London, Charles Griffin, 1975.
15. **Fonseka, J. & Mendis, K.N.** A metropolitan hospital in a non-endemic area provides a sampling pool for epidemiological studies on vivax malaria in Sri Lanka. *Transactions of the Royal Society of Tropical Medicine and Hygiene,* **81**: 360–364 (1987).
16. **Mendis, C. et al.** A method to estimate relative transmission efficiencies of anopheline species in human malaria transmission. *Journal of medical entomology*, (in press).

Annex 1

The following transfer rates were used:

$d_{i,j}$: transfer rate at time t from state $[i]$ to $[j]$; and $\bar{d}_{i,j}$: transfer rate at time $(t-\tau)$ from state $[i]$ to $[j]$, where τ is the incubation period of the malaria parasite in humans.

The variables defined below were also used in the model:

δ: vector inoculation rate at time t, as derived from eq. (H) (see Annex 2);

ε: estimated relapse rate (for one brood of parasites in the liver) (15);

α: recovery rate without retaining an extra brood of hypnozoites;

α^*: overall recovery rate, with or without retaining an extra brood of hypnozoites;

β: recovery rate while retaining an extra brood of hypnozoites;

μ_k: rate at which immune memory is lost from state $[k]$ at time t (given by eq. C); and

S: proportion of population susceptible to malaria.

Transfer rate between different states

Upon inoculation by the vector, persons whose state is negative transfer first to an incubating state at a higher immune level and then after the incubating period to a positive state (e.g., $Z_{00} \rightarrow X_{10} \rightarrow Y_{10}$).

Persons who are reinfected due to relapses transfer directly to a positive state at the same time as releasing a single brood of parasites (e.g., $Z_{01} \rightarrow Y_{10}$).

Positive cases who recover either do so completely without retaining an additional brood of parasites or recover but do retain such a brood (e.g., $Y_{10} \rightarrow Z_{10}$ or $Y_{10} \rightarrow Z_{11}$).

Persons in a negative state who lose immune memory always pass to the non-immune category (e.g., $Z_{20} \rightarrow Z_{00}$ and $Z_{10} \rightarrow Z_{00}$).

At the highest immune category (level-2), the transfer to positive states is to the same level, e.g., $Z_{21} \rightarrow X_{21} \rightarrow Y_{21}$. Below are listed expressions for the transfer rates between the various states in the model; all values are at time t, except when otherwise stated.

$$
\begin{aligned}
d_{1,14} &= \delta \cdot Z_{00}, & d_{14,17} &= \bar{d}_{1,14} \\
d_{17,11} &= \alpha \cdot Y_{10}, & d_{17,12} &= \beta \cdot Y_{10} \\
d_{11,1} &= \mu_{11}, & d_{2,15} &= \delta \cdot Z_{01} \\
d_{15,18} &= \bar{d}_{2,15}, & d_{18,12} &= \alpha \cdot Y_{11} \\
d_{18,13} &= \beta \cdot Y_{11}, & d_{12,2} &= \mu_{12} \\
d_{2,17} &= \varepsilon \cdot Z_{01}, & d_{3,16} &= \delta \cdot Z_{02} \\
d_{16,19} &= \bar{d}_{3,6}, & d_{19,13} &= \alpha^* \cdot Y_{12} \\
d_{13,3} &= \mu_{13}, & d_{3,18} &= 2\varepsilon \cdot Z_{02} \\
d_{11,24} &= \delta \cdot Z_{10} & d_{21,24} &= \delta \cdot Z_{20} \\
d_{24,27} &= (d_{11,24} + d_{21,24}), & d_{27,22} &= \beta \cdot Y_{20} \\
d_{27,21} &= \alpha \cdot Y_{20}, & d_{21,1} &= \mu_{21} \\
d_{22,27} &= \varepsilon \cdot Z_{21}, & d_{22,25} &= \delta \cdot Z_{21} \\
d_{12,25} &= \delta \cdot Z_{11}, & d_{25,28} &= (\bar{d}_{22,25} + \bar{d}_{12,25}) \\
d_{22,2} &= \mu_{22}, & d_{28,22} &= \alpha \cdot Y_{21} \\
d_{28,23} &= \beta \cdot Y_{21}, & d_{23,26} &= \delta \cdot Z_{22} \\
d_{13,26} &= \delta \cdot Z_{12}, & d_{26,29} &= (\bar{d}_{23,26} + \bar{d}_{13,26}) \\
d_{29,23} &= \alpha^* \cdot Y_{22}, & d_{23,28} &= 2\varepsilon \cdot Z_{22} \\
d_{23,3} &= \mu_{23}, & d_{12,27} &= \varepsilon \cdot Z_{11} \\
d_{13,28} &= 2\varepsilon \cdot Z_{12}.
\end{aligned}
$$

Rate of change equations for the different states

Nonimmune states:

$$
\begin{aligned}
(dZ_{00}/dt) &= d_{11,11} + d_{21,1} - d_{1,14} \\
(dZ_{01}/dt) &= d_{12,2} + d_{22,2} - d_{2,17} - d_{2,15} \\
(dZ_{02}/dt) &= d_{13,3} + d_{23,3} - d_{3,16} - d_{3,18}
\end{aligned}
$$

Immunity at level-1:

$$
\begin{aligned}
(dZ_{10}/dt) &= d_{17,11} - d_{11,1} - d_{11,24} \\
(dZ_{11}/dt) &= d_{18,12} + d_{17,12} - d_{12,25} - d_{12,2} - d_{12,27} \\
(dZ_{12}/dt) &= d_{19,13} + d_{18,13} - d_{13,3} - d_{13,26} - d_{13,28} \\
(dX_{10}/dt) &= d_{1,14} - d_{14,17} \\
(dX_{11}/dt) &= d_{2,15} - d_{15,18} \\
(dX_{12}/dt) &= d_{3,16} - d_{16,19} \\
(dY_{10}/dt) &= d_{14,17} + d_{2,17} - d_{17,11} - d_{17,12} \\
(dY_{11}/dt) &= d_{15,18} + d_{3,18} - d_{18,12} - d_{18,13} \\
(dY_{12}/dt) &= d_{16,19} - d_{19,13}
\end{aligned}
$$

Immunity at level-2:

$$
\begin{aligned}
(dZ_{20}/dt) &= d_{27,21} - d_{21,24} - d_{21,1} \\
(dZ_{21}/dt) &= d_{27,22} + d_{28,22} - d_{22,27} - d_{22,25} - d_{22,2} \\
(dZ_{22}/dt) &= d_{29,23} + d_{28,23} - d_{23,28} - d_{23,26} - d_{23,3} \\
(dX_{20}/dt) &= d_{11,24} + d_{21,24} - d_{24,27} \\
(dX_{21}/dt) &= d_{12,25} + d_{22,25} - d_{25,28} \\
(dX_{22}/dt) &= d_{13,26} + d_{23,26} - d_{26,29} \\
(dY_{20}/dt) &= d_{12,27} + d_{24,27} + d_{22,27} - d_{27,22} - d_{27,21} \\
(dY_{21}/dt) &= d_{25,28} + d_{13,28} + d_{23,28} - d_{28,23} - d_{28,22} \\
(dY_{22}/dt) &= d_{26,29} - d_{29,23}
\end{aligned}
$$

S is defined such that the sum of all X, Y, and $Z = S^*$ (total population).

Annex 2

There are three states of the vector: negative (susceptible to infection), incubating and positive for sporozoites. The proportion of vectors in these three states at time t are $W_1(t)$, $W_2(t)$, and $W_3(t)$, respectively (Fig. 2).

The following are defined:

a: man biting habit;

$\hat{\tau}$: incubating period between intake of a gametocyte and the development of a sporozoite;

s_0: probability of a successful infection, given that an infective mosquito bites a "susceptible" human (without the effect of transmission-blocking immunity);

$J_1(t)$: average relative infectivity of individuals at level-1 of transmission-blocking immunity at time t (from eq. B);

$J_2(t)$: average relative infectivity of individuals at level-2 of transmission blocking immunity at time t (from eq. B);

s_1: the probability of a "successful" intake of parasite into a mosquito that has bitten an infectious human.

If V_1 and V_2 are the proportion of humans infective at level-1 and level-2, respectively, then

$$V_1(t) = \sum_{j=0}^{2} Y_{1j}(t)/N,$$

and

$$V_2(t) = \sum_{j=0}^{2} Y_{2j}(t)/N$$

where N is the total human population.

m: daily mortality rate, which is assumed to be constant.

If we denote any evaluations at time $(t - \hat{\tau})$ by a bar above the function, and those at time t with no bar, i.e.,

$$V_1(t - \hat{\tau}) = \bar{V}_1 \quad \text{and} \quad V_1(t) = V_1$$

then for the positive state,

$$(dW_3/dt) = as_1(\bar{J}_1\bar{V}_1 + \bar{J}_2\bar{V}_2)W_1 \exp[-m\hat{\tau}] - mW_3 \quad (F)$$

and for the incubating state,

$$(dW_2/dt) = as_1(J_1V_1 + J_2V_2)W_1 - as_1(J_1V_1 + J_2V_2)W_1 \exp[-m\hat{\tau}] - mW_2 \quad (G)$$

and we have

$$W_1 + W_2 + W_3 = 1 \quad (H)$$

The sporozoite rate $SPR(t) = W_3(t)$, hence the inoculation rate, assuming a Poisson distribution with a mean frequency of $(Mbr \times SPR)$, where Mbr = man-biting rate, is given by

$$\delta(t) = s_0(1 - \exp[-Mbr \times W_3(t)]) \quad (I)$$

Effective man-biting rate

An equivalent Mbr is defined as $Mbr = \sum_{i=1}^{p} e_{ik}(Mbr)_i$, where e_{ik} is transmission efficiency of an ith species with respect to a kth species; $(Mbr)_i$ is the man-biting rate of the ith species, and p is total number of species detected with sporozoites. Values for e_{ik} are shown in the Table.

Table: **Relative transmission efficiency values, e_{ik}, for various species of mosquito**

	Species[a]					
	A.cul	A.nig	A.pal	A.sub	A.tes	A.vag
$\overline{e_{ik}}$	1.00	0.89	0.29	0.77	1.75	0.48

[a] A.cul = *Anopheles culicifacies*, A.nig = *A. nigerrimus*, A.pal = *A. pallidus*, A.sub = *A. subpictus*, A.tes = *A. tessellatus*, A.vag = *A. vagus*.

Vector properties

The vector properties of *A. culicifacies* used for the simulation are shown below.

Daily mortality rate (m) = 0.198 (measured from field observations).

Mean man-biting habit, dry season = 0.32 (data not shown).

Mean man-biting habit, wet season = 0.20 (data not shown).

Incubating period ($\hat{\tau}$) = 9 days (laboratory observation).

Annex 3

The terms in eq. E for different states of loss of immune memory for boosting are shown in the Table.

Table: **Terms in eq. *E* (see text)**

k^*[a]	$\mu_k = ZO(t)$	$ZI(t)$[b]	$\Theta(t)$[c]
11	μ_{11}	$\alpha \cdot Y_{10}$	δ
12	μ_{12}	$\alpha \cdot Y_{11} + \beta \cdot Y_{10}$	$\delta + \varepsilon$
13	μ_{13}	$\alpha^* \cdot Y_{12} + \beta \cdot Y_{11}$	$\delta + 2\varepsilon$
21	μ_{21}	$\alpha \cdot Y_{20}$	δ
22	μ_{22}	$\alpha \cdot Y_{21} + \beta \cdot Y_{20}$	$\delta + \varepsilon$
23	μ_{23}	$\alpha^* \cdot Y_{22} + \beta \cdot Y_{21}$	$\delta + 2\varepsilon$

[a] k^* = states as shown in Fig. 1.

[b] α = (1 − proportion relapsing)/(time span of disease); α^* = 1/(time span of disease); β = (proportion relapsing)/(time span of disease).

[c] ε = relapse rate (estimated from ref. *15*); all values are at time t.